Hindawi Publishing Corporation
Advances in OptoElectronics
Volume 2012, Article ID 313984, 11 pages
doi:10.1155/2012/313984

Review Article

Dirac Dispersion in Two-Dimensional Photonic Crystals

C. T. Chan, Zhi Hong Hang, and Xueqin Huang

Department of Physics, Hong Kong University of Science and Technology, Clear Water Bay, Kowloon, Hong Kong

Correspondence should be addressed to C. T. Chan, phchan@ust.hk

Received 6 July 2012; Accepted 6 September 2012

Academic Editor: Pavel A. Belov

We show how one may obtain conical (Dirac) dispersions in photonic crystals, and in some cases, such conical dispersions can be used to create a metamaterial with an effective zero refractive index. We show specifically that in two-dimensional photonic crystals with C_{4v} symmetry, we can adjust the system parameters to obtain accidental triple degeneracy at Γ point, whose band dispersion comprises two linear bands that generate conical dispersion surfaces and an additional flat band crossing the Dirac-like point. If this triply degenerate state is formed by monopole and dipole excitations, the system can be mapped to an effective medium with permittivity and permeability equal to zero simultaneously, and this system can transport wave as if the refractive index is effectively zero. However, not all the triply degenerate states can be described by monopole and dipole excitations and in those cases, the conical dispersion may not be related to an effective zero refractive index. Using multiple scattering theory, we calculate the Berry phase of the eigenmodes in the Dirac-like cone to be equal to zero for modes in the Dirac-like cone at the zone center, in contrast with the Berry phase of π for Dirac cones at the zone boundary.

1. Introduction

The Dirac equation is the wave equation formulated to describe relativistic spin 1/2 particles [1]. In the special case where the effective mass of the spin 1/2 particle is zero, and the solution to Dirac equation has a linear dispersion in the sense that the energy E is linearly proportional to the wave vector k. The electric band structure of graphene near the Fermi level can be described by the massless Dirac equation and hence exhibit the Dirac dispersion [2–15]. The electronic band dispersion is linear near the six corners of the two-dimensional (2D) hexagonal Brillouin zone at the K and K' points, and the dispersion close to the Fermi energy at each of these corner k-points can be visualized as two cones meeting at the Fermi level at one point called the Dirac point, and the conical dispersion near the Dirac point is usually referred to as Dirac cones. This rather singular electronic band structure of graphene near the Fermi level gives rise to many unusual transport properties [2–15], including quantum hall effect [4–6], Zitterbewegung [7–11], and Klein paradox [12]. Dirac cone dispersions are not limited to graphene but can also be found in classical wave periodic systems such as photonic crystals [16–24]. In fact, linear dispersions at the Brillouin zone boundary for 2D triangular photonic crystals appeared in the photonic band gap literature a long time ago [16] except that the attention at that time was focused on the creation of band gaps [25–27] and as Dirac points are by definition gapless, their existence was largely ignored. The special properties of such conical dispersions at the zone boundary of triangular photonic crystals were not explicitly noted until much later [21, 22]. It was noted that if an external magnetic field is used to break time reversal symmetry, unidirectional and backscattering immune electromagnetic wave propagation, analogous to quantum hall edge states, can be realized, and such ideas were indeed demonstrated subsequently using photonic crystals constructed with gyromagnetic materials [21–24, 28–32]. In 2D, the acoustic wave equation has the same form as the Maxwell equation for one polarization, and it follows immediately that Dirac cone dispersions can also be realized in acoustic wave crystals [33]. In fact, some intriguing wave transport phenomena such as Zitterbewegung is the consequence of the Dirac dispersion and hence can be realized in 2D photonic [20] and phononic crystal [33], and such effects were indeed numerically demonstrated [20] and experimentally verified [33]. With much longer wavelength compared to electrons, and without the complication of electron-electron interaction, photonic, and phononic

crystals have become an ideal platform to study various interesting wave propagation properties related to Dirac dispersion.

It turns out that the Dirac dispersion has interesting relationship with metamaterials, which are artificial composite materials that have novel wave manipulation capabilities. Since the theoretical proposal of materials with negative refractive indices proposed by Veselago in 1968 [34] and the first demonstration of a material with both effective permittivity (ε_{eff}) and effective permeability (μ_{eff}) less than zero in 2001 [35], metamaterials with all kinds of effective permittivity (ε_{eff}) and effective permeability (μ_{eff}) not found in nature have been designed and realized [35–48]. With the help of these metamaterials, many interesting waveguiding properties, some seemingly fictional, have been achieved including negative refraction [35–39], superlens [40, 41], cloaking [42–44], field concentrators [45], superscatterer [46], field rotators [47], and illusion optics [48]. While previous attention may have been focused on realizing metamaterials with negative refractive indices, materials that have zero refractive indices are equally interesting. As $n^2 = \varepsilon\mu$, a zero-refractive-index material can have either single zero ($\varepsilon_{\text{eff}} = 0$ or $\mu_{\text{eff}} = 0$) or double zero ($\varepsilon_{\text{eff}} = \mu_{\text{eff}} = 0$) [49–64]. There is no phase variance in the wave transport process inside a zero-index material. This leads to many peculiar properties such as the tunneling of electromagnetic waves through subwavelength channels and bends [49–57], the tailoring of the radiation phase pattern of arbitrary sources [58–60], and the cloaking of objects inside a channel with specific boundary conditions [61–64]. The tunneling phenomenon has been demonstrated experimentally using complementary split ring resonators at the microwave frequency [55]. However, the impedance mismatch is typically huge for single-zero materials, and the incident wave may encounter reflection when the aperture of the waveguide is larger than wavelength [60, 64]. This problem can be mitigated if we use double-zero material ($\varepsilon_{\text{eff}} = 0$ and $\mu_{\text{eff}} = 0$ at the same frequency).

While Dirac cone dispersion and zero-index materials may seem unrelated, there is a subtle relationship between them. If we have a homogeneous material with isotropic dispersive permittivity $\varepsilon(\omega)$ and permeability $\mu(\omega)$ at a particular frequency ω_0 and $\varepsilon(\omega_0) = \mu(\omega_0) = 0$, the dispersion near ω_0 will have a linear dispersion, $\omega = \omega_0 + v_g k$, where k is the wave vector and v_g is the corresponding group velocity [65]. This linear dispersion and the associated conical dispersion are different from the Dirac dispersion found in graphene [2–15] or hexagonal photonic/phononic crystals [16–24, 31–33] as the Dirac point is not at the Brillouin zone boundary but at the zone center. This relationship opened a new window to the physics related to Dirac cones but the question is whether we can construct a metamaterial with $\varepsilon(\omega_D) = \mu(\omega_D) = 0$ at a particular frequency ω_D using a conical dispersion at $k = 0$ close to this frequency. Another important issue is that a homogenous $\varepsilon(\omega_0) = \mu(\omega_0) = 0$ implies a Dirac cone dispersion but the converse may not be true for the simple reason that an effective medium description may or may not be applicable to the composite material with a Dirac cone dispersion. We will show by examples that there are indeed systems which have Dirac-like cone at $k = 0$, and we will examine the conditions for effective medium theory to be applicable [66].

We will show that if a 2D photonic crystal has C_{4v} symmetry, we can obtain accidental degeneracy of a twofold degenerate state and a nondegenerate state at Γ point by tuning the parameters of the structure, and that two of the states of the triply degenerate state have linear dispersions near Γ, and they can generate conical dispersions. We will further demonstrate that if the triply degenerate state is derived from monopole and dipole excitations, we can use effective medium theory to map this photonic crystal to a zero-index material with both permittivity and permeability equal to zero simultaneously [66]. We will also give examples that conical dispersions at the zone center can be obtained for situations in which the bands are not derived from monopole and dipole excitations, and in these cases, we will demonstrate that these Dirac-like cone systems cannot be related to an effective medium with a zero refractive index. In this paper, we will also examine the Berry phase [67] associated with the Dirac-like cone at $k = 0$ which is the phase acquired by the eigenvector over a cyclic evolution in k space about the Dirac point. It is known that the Berry phase associated with the Dirac cone is π in electronic graphene and has very subtle implications in wave function transport properties [4–6]. We will show that the Berry phase associated with the Dirac-like cone at Γ point is different from that of graphene because of the existence of an additional quasi-longitudinal mode. The paper is organized as follows. In Section 2, we introduce the Dirac-like point at Γ point and M point in 2D photonic crystal with C_{4v} symmetry and examine the possibility and consequences of effective medium descriptions. In Section 3, we calculate the Berry phase of the triply degenerate state formed by Dirac-like point. We will then give a summary.

2. Dirac-Like Point at Γ Point and M Point in C_{4v} Symmetry

Let us first consider an example of a 2D photonic crystal that exhibits a Dirac-like cone in the zone center and in this specific structure, effective medium theory can be used to relate the system to an effectively zero-refractive-index system [66]. The photonic crystal is a square array of alumina cylinders with relative permittivity $\varepsilon = 8.8$ in air and the polarization is transverse-magnetic (TM) polarization, with electric field parallel to the cylinder axis. The radii of the cylinders are $0.221a$, where a is the lattice constant. There is a triply degenerate state at a frequency ω_D at the Γ point. We note that the triple degeneracy is not a consequence of lattice symmetry in the sense that if we choose other system parameters (e.g., a different cylinder radius), the triple degenerate state will split into a doublet and a singlet. The field patterns of these three states are shown in Figures 1(d)–1(f). We see that electromagnetic field is mostly confined inside the high refractive index rod and two of the eigenmodes (panels (e) and (f)) have a strong dipolar character, with the wave vector perpendicular/parallel to

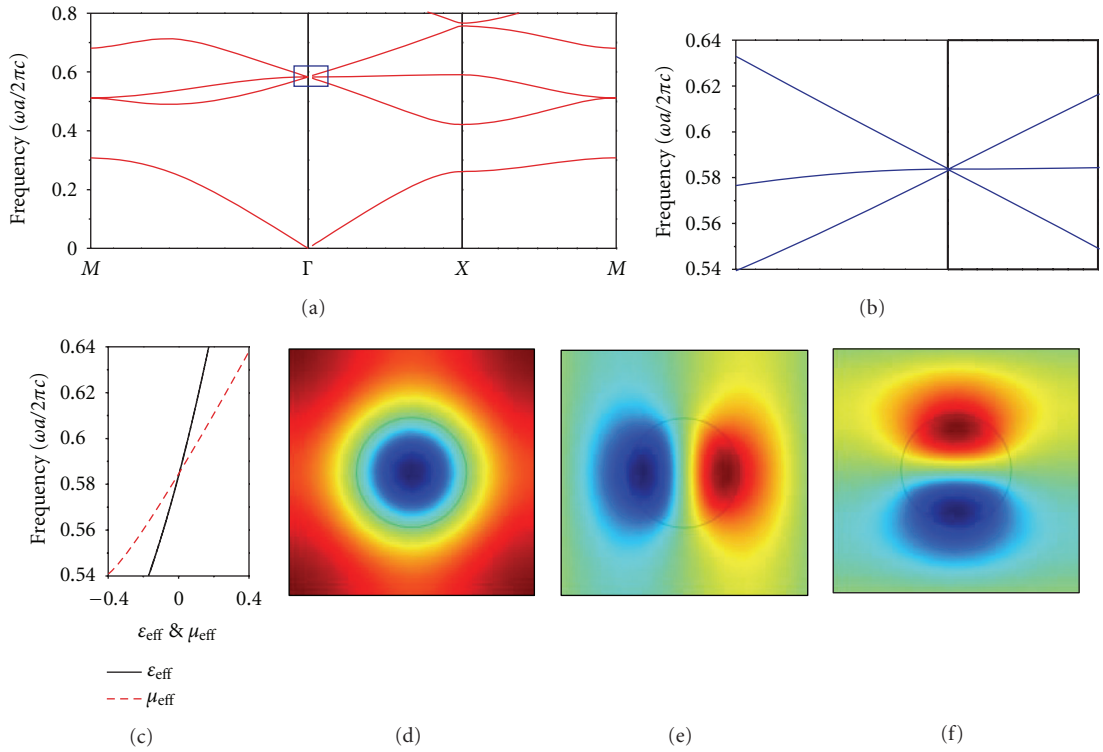

FIGURE 1: (a) The band structure of a two-dimensional photonic crystal composing of alumina cylinders arranged in a square lattice for the TM polarization. The radii of the cylinders are $0.221a$. The relative permittivity of the cylinders is 8.8. At the Γ point, a triply degenerate state is formed, and the linear dispersion near the zone center is highlighted in (b). (c) The effective permittivity ε_{eff} (black solid line) and permeability μ_{eff} (red dash line) of this alumina photonic crystal. Note that $\varepsilon_{\text{eff}} = \mu_{\text{eff}} = 0$ at the Dirac-like point. (d)–(f) The field patterns of the three eigenmodes near the Dirac-like point with a very small k along ΓX direction.

the dipole moment (transverse/longitudinal dipole mode), and the other eigenmode has a monopole character. By examining carefully the band diagram near ω_D ((Figure 1(b)) corresponding to the solid blue region in Figure 1(a), we found that the two linear bands generate a conical dispersion with the upper and lower cones touching at a Dirac-like point at ω_D. The equifrequency contours are circular near ω_D and eigenmodes in the cones are linear combinations of transverse dipole and monopole modes. There is an extra flat band intersecting the Dirac-like cones at ω_D. The modes in this flat sheet of states are quasi-longitudinal such that the magnetic field is mostly parallel to the k-vector. It can be shown [68] that if the band dispersions in a 2D photonic crystal can be described by monopole and dipole interactions, an effective medium theory [68] can be applied to extract effective constitutive parameters and when these parameters of the photonic crystal are retrieved, we find that $\varepsilon_{\text{eff}}(\omega_D) = \mu_{\text{eff}}(\omega_D) = 0$ at the Dirac frequency ω_D (Figure 1(c)). The sheet of quasi-longitudinal modes cutting through the Dirac-like point corresponds to the longitudinal solution to the Maxwell equation when $\mu_x = \mu_y = 0$ for TM polarization (or $\varepsilon_x = \varepsilon_y = 0$ for TE polarization). For a homogenous isotropic medium with $\varepsilon = \mu = 0$, this longitudinal mode has exactly zero group velocity but in a composite system, this mode has a quadratic dispersion far away from the zone center because of spatial dispersion.

In order to demonstrate that the photonic crystal with a band dispersion shown in Figure 1 does have $\varepsilon_{\text{eff}}(\omega_D) = \mu_{\text{eff}}(\omega_D) = 0$ at the Dirac frequency, numerical simulations, and microwave experiments were carried out [66]. Both the focusing effect through a concave lens and the waveguiding and cloaking effect through a waveguide filled with $\varepsilon_{\text{eff}} = \mu_{\text{eff}} = 0$ photonic crystal were demonstrated. The $\varepsilon_{\text{eff}} = \mu_{\text{eff}} = 0$ photonic crystal was demonstrated to have nearly the same field distributions as a homogenous $\varepsilon = \mu = 0$ medium in wave transport simulations. For example, as there is no phase change during the propagation through a zero-index material, the zero-index material can serve as a wavefront transformer [58–60]. Here, we numerically demonstrate another wavefront transformer phenomenon, the transformation of a Gaussian beam to a plane wave. In Figure 2(a), an $18a \times 18a$ block of a hypothetical homogeneous $\varepsilon = \mu = 0$ medium is put inside a waveguide and is illuminated with a tightly focused Gaussian beam whose waist is equal to $3a$, where a is the lattice constant of the photonic crystal shown in Figure 1. As the only allowed propagation mode through a homogeneous $\varepsilon = \mu = 0$ medium is a plane wave with zero parallel wavevector and as the exit surface is flat, the wave leaving the exit surface should be a plane wave with equal phase at the exit surface as demonstrated numerically in Figure 2(a). The field inside the homogeneous $\varepsilon = \mu = 0$ medium is constant. In Figure 2(b), we replace the

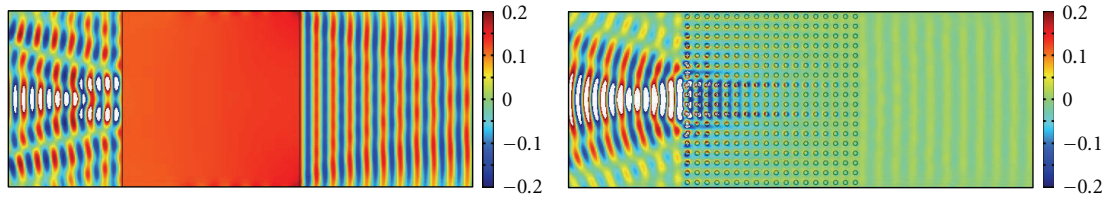

(a) (b)

Figure 2: Numerical simulation that demonstrates the $\varepsilon_{\text{eff}} = \mu_{\text{eff}} = 0$ property of the alumina photonic crystal with Dirac-like cone dispersion at the Brillouin zone center. (a) An $18a \times 18a$ block of a hypothetical homogeneous $\varepsilon = \mu = 0$ medium is placed inside a waveguide with a tightly focused (waist equal to $3a$) Gaussian beam incident at the surface of the homogeneous$\varepsilon = \mu = 0$ medium. As the $\varepsilon = \mu = 0$ medium only allows plane wave with $k_{\parallel} = 0$ to propagate, we expect only plane wave can exit, which can be clearly seen. The Gaussian wave front is transformed to a plane wave. (b) By replacing the homogeneous $\varepsilon = \mu = 0$ medium with the $\varepsilon_{\text{eff}} = \mu_{\text{eff}} = 0$ alumina photonic crystal, very similar wavefront transformation can be observed. Here, a is the lattice constant of the photonic crystal.

homogeneous $\varepsilon = \mu = 0$ medium with the photonic crystal consisting of alumina cylinders, and we observe a similar transformation of a Gaussian wave to a plane wave. The field distributions inside the photonic crystal are slightly different from the homogeneous $\varepsilon = \mu = 0$ medium shown in Figure 2(a) due to the excitation of the quasi-longitudinal mode in the photonic crystal.

The realization of $\varepsilon_{\text{eff}} = \mu_{\text{eff}} = 0$ using dielectric photonic crystals may enable us to achieve various waveguiding applications specific to zero-refractive-index medium in the near future. There are multiple ways to realize a zero refractive index. For example, $\varepsilon_{\text{eff}} = 0$ or $\mu_{\text{eff}} = 0$ or $\varepsilon_{\text{eff}} = \mu_{\text{eff}} = 0$ metamaterial can be designed and fabricated using metallic resonant structures [55]. However, metallic resonant structure is always lossy, and the loss will become more severe when at higher frequencies. On the other hand, as the photonic crystals with Dirac-like cone at $k = 0$ are made with dielectric, the system can function as $\varepsilon_{\text{eff}} = \mu_{\text{eff}} = 0$ system with small material loss all the way up to optical frequencies and the fabrication of nanoscale dielectric pillar structure is feasible with modern silicon nanofabrication technology [69]. We also remark that the Dirac-like cone at $k = 0$ gives us $\varepsilon_{\text{eff}} = 0$ and $\mu_{\text{eff}} = 0$ simultaneously ("double zero") which has the advantage of a finite group velocity and favorable impedance matching as compared to a "single zero" material ($\varepsilon_{\text{eff}} = 0$ or $\mu_{\text{eff}} = 0$ but not both) which has a zero group velocity and poor impedance matching. The double-zero condition is difficult to satisfy if we use metallic resonators to obtain $\varepsilon_{\text{eff}} = 0$ and $\mu_{\text{eff}} = 0$ at the same frequency.

As the necessary (but not sufficient) condition to get an $\varepsilon_{\text{eff}} = \mu_{\text{eff}} = 0$ photonic crystal is a Dirac-like cone at $k = 0$ and the condition to get a Dirac-like cone at the zone center is accidental degeneracy, we will discuss here how to obtain accidental degeneracy, and we limit our discussion here to square lattice systems. The point group symmetry of a photonic crystal of square array of cylinders belongs to the C_{4v} group [70]. The irreducible representations of C_{4v} point group are A_1, B_1, A_2, B_2, and E, where A_1, B_1, A_2, B_2 are nondegenerate representations, and E is a doubly degenerate representation. The eigenstates at $k = 0$ of a square lattice photonic crystal should have symmetries related to these irreducible representations. At a finite frequency, the dispersion of a nondegenerate band at Brillouin zone center has to be parabolic as required by time reversal symmetry [71–73]. However, we need linear bands to generate Dirac-like cones. Linear dispersion at the Brillouin zone center (Γ point) can emerge as a consequence of accidental degeneracy of states which are not required by lattice symmetry to be equal in frequency and such accidental degeneracy can be obtained by tuning the dielectric constant or the radii of the cylinders in 2D photonic crystals.

For a periodic structure with a permittivity distribution $\varepsilon(\vec{r})$, the Bloch eigenfunction $\psi_k(\vec{r})$ should satisfy the equation

$$\nabla \times \left[\frac{1}{\varepsilon\left(\vec{r}\right)} \nabla \times \psi_k\left(\vec{r}\right) \right] = \frac{\omega_k^2}{c^2} \psi_k\left(\vec{r}\right), \tag{1}$$

where $\psi_k(\vec{r})$ is the eigenmode of the magnetic field and ω_k is the corresponding eigenvalue. The Bloch eigenfunction can be chosen to a linear combination of the localized states (e.g., Wannier-type function) of A_1, B_1, A_2, B_2, E representations of the C_{4v} point group [72–75] centered on the cylinders. It can be written as

$$\psi_k\left(\vec{r}\right) = \frac{1}{V} \sum_{l,\, m} e^{i\vec{k}\cdot\vec{r}_{lm}} \sum_i A_i M^{(i)}\left(\vec{r} - \vec{r}_{lm}\right), \tag{2}$$

where $\vec{r}_{lm} = la\hat{x} + ma\hat{y}$, a is the lattice constant. V is the volume of the unit cell. $M^{(i)}(\vec{r})$ are localized functions of A_1, B_1, A_2, B_2, E representations, where i labels the irreducible representation. These basis functions are chosen to be orthogonal

$$\int_V d\,\vec{r}\; M^{(i)^*}\left(\vec{r}\right) \cdot M^{(j)}\left(\vec{r}\right) = V\delta_{ij}. \tag{3}$$

The integral is over the whole unit cell V.

These basis functions have different symmetry properties. For instance, modes of the A_1 representation invariant for all symmetry operation and if a band is derived from the

monopole excitations of the cylinders, it should be expanded by $M^{A_1}(\vec{r})$. As modes of E representations have mirror symmetry about the x- and y-axis, respectively, $M^E_{1,2}(\vec{r})$ can be used to expand bands that derived from dipole excitations of the cylinders in the photonic crystals. We can obtain a "double-zero" photonic crystal if we design the system to have accidental degeneracy so that the monopole and dipole derived bands become degenerate at the zone center. In that case, the eigenmodes near the zone center should be expressed as a linear combination of $M^{A_1}(\vec{r})$ and $M^E_{1,2}(\vec{r})$ states. Generally speaking, if there is accidental degeneracy at the zone center, the eigenmodes will be a combination of two irreducible states, either a mix of three states (for the case of E state degenerate with any nondegenerate state) or a mix of two states (the degeneracy of two nondegenerate states). For simplicity, we only consider the accidental degeneracy of E state and A_1 state. If we only consider the nearest neighbor interaction, $l, m = 0, \pm 1$, multiply $M^{(i)^*}(\vec{r})$on both side of (1), integrate over the unit cell V, and use orthogonal condition of (3), we can transfer (1) into a secular equation

$$\left| \overleftrightarrow{S} - \frac{\omega_D^2}{c^2} \overleftrightarrow{I} \right| = 0. \tag{4}$$

$\overleftrightarrow{S}$ is a 3×3 matrix with $S_{ij} = \sum_{lm} e^{ia(lk_x + mk_y)} L^{ij}_{lm}$, where $L^{ij}_{lm} \equiv (1/V) \int_V d\ \vec{r}\ M^{(i)^*}(\vec{r}) \cdot \nabla \times [(1/\varepsilon(\vec{r}))\nabla \times M^{(j)}(\vec{r} - \vec{r}_{lm})]$ is a transfer integral. ω_D is the accidental degeneracy frequency. $M^{(i/j)}$ can be either M^{A_1} or $M^E_{1,2}$. By solving (4) close to the Γ point, with tiny k_x and k_y, the dispersion near ω_D can be found consisting of two linear bands with a finite group velocity along with a quadratic band which is very flat near the Γ point. The linear bands will generate conical dispersion (Dirac cone) close to the degeneracy frequency ω_D near the Γ point. The degenerate frequency ω_D is the Dirac-like point frequency we are looking for. We note that the emergence of linear bands as a consequence of accidental degeneracy at $k = 0$ can also be obtained using multiple scattering theory [66] or $k \cdot p$ perturbation [76, 77]. Conical dispersions will also emerge from the accidental degeneracy of E states and the other three nondegeneracy states B_1, A_2, B_2. The linear bands giving rise to conical dispersion will always be accompanied by a quadratic band if the accidental degeneracy is threefold.

We now have a recipe to create Dirac dispersion at a finite frequency at $k = 0$ for the lattice with C_{4v} point group symmetry. However, we should emphasize that Dirac dispersion is a necessary but not sufficient condition to obtain $\varepsilon_{\text{eff}} = \mu_{\text{eff}} = 0$. As we are always dealing with composite materials with at least two components, an effective medium theory must be applied to extract the effective constitutive parameters from the optical properties of the discrete system. For photonic applications, we prefer to use "local" effective parameters which depend only on the frequency but not the wave vector. The Dirac cones that are discussed in the literature are located at the Brillouin zone boundary [16–24] and at such a large wave vector, no effective medium theory can be applied reliably. Even at the Γ point, effective medium theory can be applicable only if certain conditions are satisfied. It can be shown that in 2D photonic crystals, effective medium theory can be applied to extract ε_{eff} and μ_{eff} if the bands are derived from the monopole and dipole scattering of the building blocks [68], and this condition is indeed satisfied by the photonic crystal system shown in Figures 1 and 2. This condition can typically be satisfied in photonic crystals comprising dielectric cylinders in air in which the low-lying bands are formed by the scattering of monopole and dipole excitations of the individual dielectric cylinders, and the field distributions of the eigenmodes tend to be confined in the cylinders. If the eigenmodes have projections on higher multipoles, the effective medium description will not be good. This can happen if the dielectric constant of the cylinders is small so that Dirac-like cone appears at high frequencies. Also, if we have an inverted structure, such as photonic crystals with cylindrical holes drilled in high dielectric background medium, the effective medium will naturally fail as the eigenmodes in those situations typically have large projections on high multipoles centered on the holes.

From symmetry considerations, we know that as long as there is an accidental degeneracy of a doubly degenerate state with a nondegenerate state, the Dirac-like point can be formed. And we have already shown in Figure 1 that Dirac-like cones can be formed when there is accidental degeneracy of monopole and dipole modes that are described by E and A_1 representations, and the photonic crystal behaves like a zero-index material near the Dirac-like point. Here, we give an example of a photonic crystal which has a Dirac-like point that is formed by the accidental degeneracy of eigenmodes of E and B_1 representations. The system consists of core-shell cylinders arranged in a square lattice and the band structure for the TE polarization with the magnetic field along the cylinder axis is shown in Figure 3(a). The radii of the shell and core are $R_{\text{shell}} = 0.4a$ and $R_{\text{core}} = 0.181a$ respectively. Here, a is the lattice constant. The relative permittivity of the shell and core $\varepsilon_{\text{shell}} = 11.75$ and $\varepsilon_{\text{core}} = 1$. There is a Dirac-like point at the Γ point at the location highlighted by the blue box, comprising of two linear bands and a flat band cross intersecting at the same frequency (Figure 3(a)). The enlarged band structure near the Dirac-like point is shown in the inset. In order to understand the underlying physics, we plot the eigenmodes of this triply degenerate state in Figures 3(b) to 3(d). Figures 3(b) and 3(c) show that the eigenmode has strong dipole character, and Figure 3(d) shows a quadrupole excitation. Symmetry analysis shows that the dipole excitations belong to the E representation, while the quadrupole excitation belongs to the B_1 representation. As effective medium theory [68] is not expected to work when the bands have a strong quadrupole character, we expect that the system should not behave like a zero-index medium even though it has a conical dispersion. To see the wave transport properties of this system near the Dirac frequency, a Gaussian beam is illuminated to this photonic crystal as shown in Figure 3(e), with the same parameters as in Figure 2(b). There are phase changes inside the photonic crystal, and the field distributions outside are

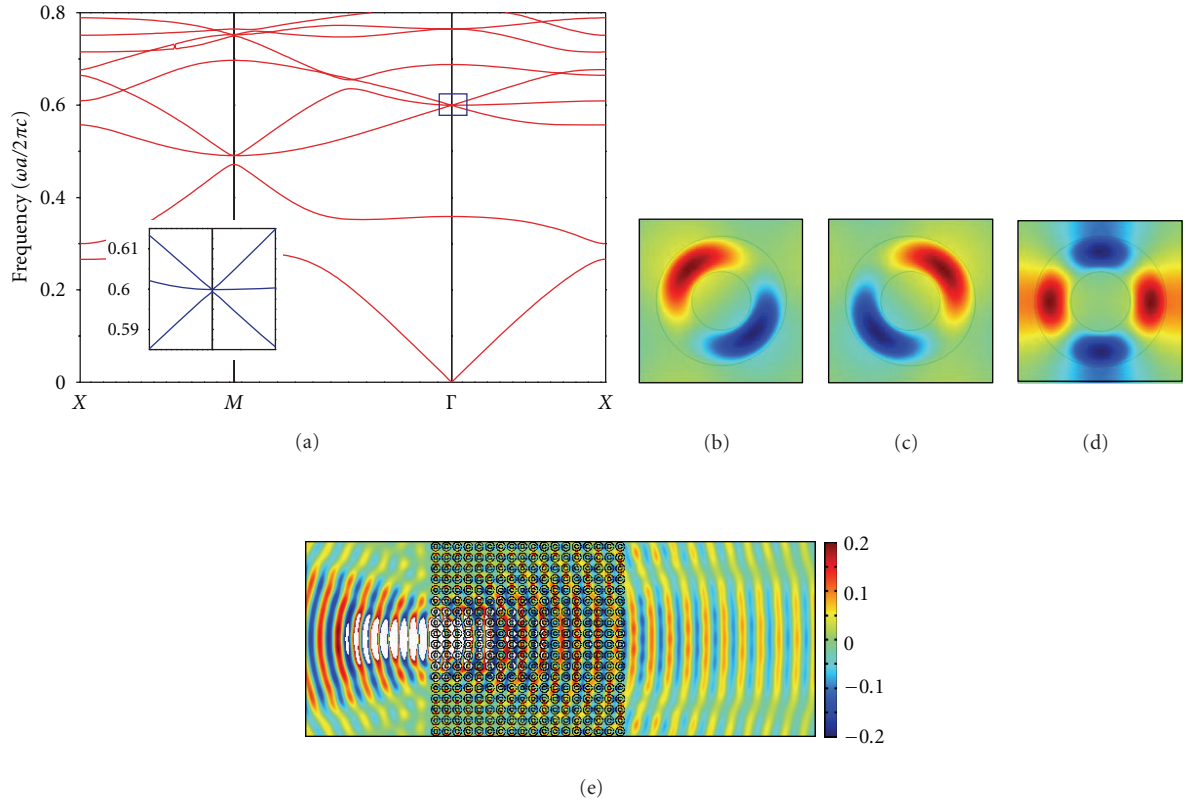

FIGURE 3: (a) The band structure of a core-shell photonic crystal arranged in square lattice for the TE polarization. The radii of the shell and core to be $R_{\text{shell}} = 0.4a$ and $R_{\text{core}} = 0.181a$. The relative permittivity of the shell and core are $\varepsilon_{\text{shell}} = 11.75$ and $\varepsilon_{\text{core}} = 1$. Near the Γ point, there is a Dirac-like cone dispersion. The inset is the enlarged part near the Dirac-like point shown by blue solid region. (b)–(d) The eigenmodes of the photonic crystal at the Γ point. (b) and (c) dipole excitations, (d) quadrupole excitation. (e) As effective medium theory cannot be applied here, the crystal cannot be mapped to a $\varepsilon_{\text{eff}} = \mu_{\text{eff}} = 0$ system and hence the field distributions for an incident Gaussian beam deviate from what is expected for homogeneous $\varepsilon = \mu = 0$ medium (Figure 2(a)).

not a plane wave front. The wave transport behavior deviates from what is expected from an $\varepsilon = \mu = 0$ medium.

For completeness, we also show the properties of photonic crystals consisting of low dielectric cylinders and we examine whether such systems can be used to mimic a $\varepsilon_{\text{eff}} = \mu_{\text{eff}} = 0$ material. We use a low dielectric constant material, PMMA with $\varepsilon = 2.6$ for the cylinders. We can adjust the structural parameters to obtain accidental degeneracy and Dirac-like cone dispersion can be achieved as shown in Figure 4(a). A Dirac-like cone is obtained when the radii of the cylinders are $0.3035a$. The band structure is shown for the TM polarization in Figure 4(a). When we repeat the same simulation as in Figure 2(b) for this PMMA photonic crystal, the wavefront transformation effect (Figure 4(b)) is also different to what is expected from homogeneous $\varepsilon = \mu = 0$ medium. In this low dielectric contrast system, the low-lying bands are better described by a plane wave basis rather than the coupling of localized modes centered on a cylinder. Alternatively, one may say that the Dirac-like cone will be found at high frequencies if the dielectric cylinders have a low refractive index and effective medium theory has to fail at high frequencies. In fact, calculations show that the effective medium description gets better and better if the cylinders have progressively higher dielectric constants with the corresponding Dirac-like cone moving to lower frequencies.

Some remarks are in order here. We note that the band dispersion is not just linear in one direction, but it is isotropic and linear in all directions of k-vectors and as such, the isotropic linear dispersion generates two cones that touch at one point commonly referred to a Dirac point. The Dirac cone dispersion in graphene is generated by two degrees of freedom, frequently formulated as two components of a pseudospin. These two degrees of freedom are actually the amplitude of the p_z wave functions on sites A and B of the carbon atoms within the unit cell of graphene. In the Γ point Dirac cone in photonic crystals, we actually have three degrees of freedom, two from the dipolar excitations and one from the monopolar excitation. These three freedoms generate a conical dispersion plus a flat band. We also remark that not all linear dispersions form Dirac cone/Dirac point. For example, most classical wave systems have linear dispersions in the limit of $\omega \to 0$, but this is not a Dirac cone as the negative frequency solution has no physical meaning.

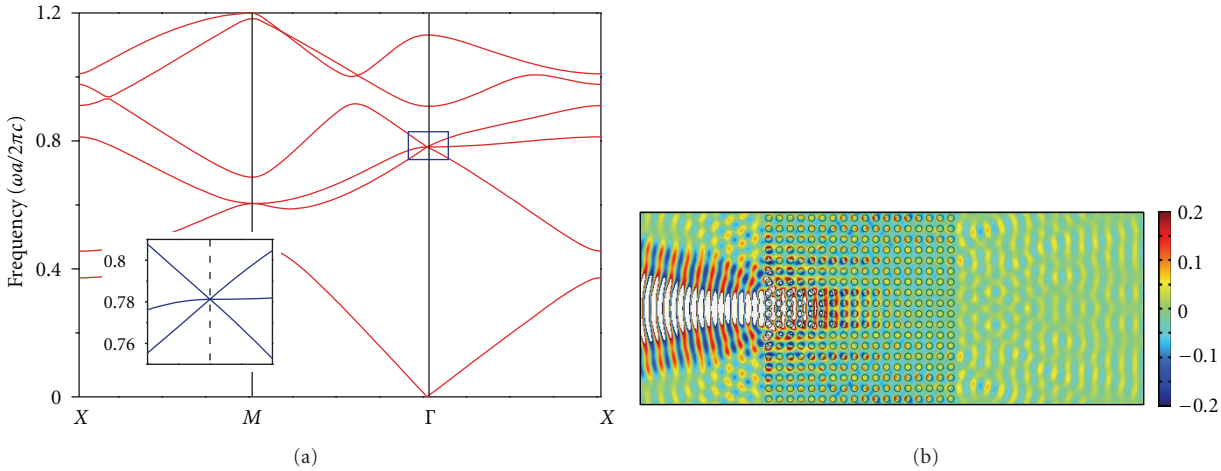

FIGURE 4: (a) The band structure of PMMA photonic crystal arranged in a square lattice for the TM polarization. The radii of the cylinders are $0.3035a$. The relative permittivity of the PMMA is 2.6. Near the Γ point, there is also a Dirac-like cone dispersion. The inset is the enlarge part near the Dirac-like point shown by blue solid region. (b) The field distributions for a Gaussian beam illumination. The Gaussion beam parameters are the same as in Figure 2.

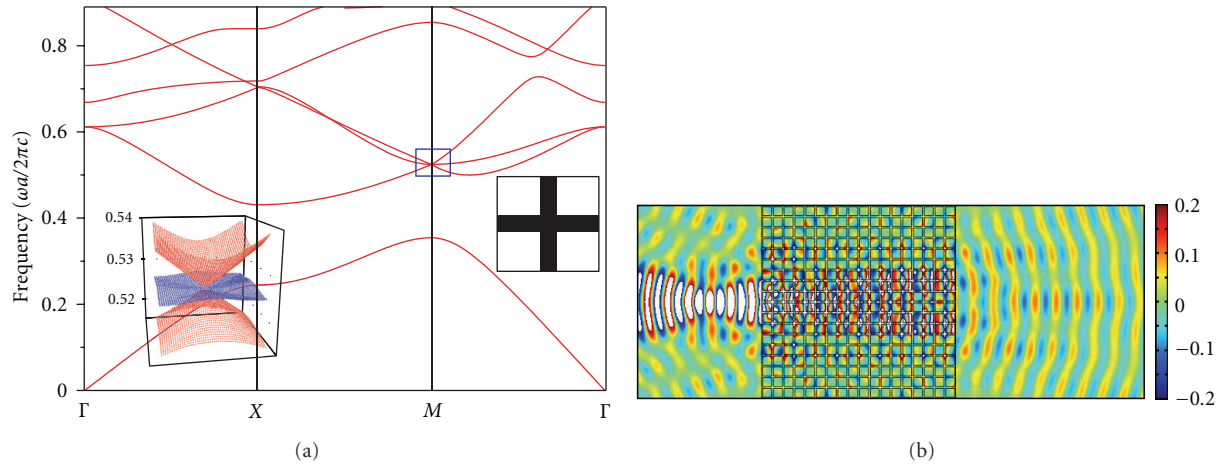

FIGURE 5: (a) The band structure of a alumina vein structure for the TE polarization, with the thickness of the vein equal to $0.176a$. At the M point, a conical dispersion intersects with an extra sheet. A closeup of the band diagram contour of the blue solid region is shown in the inset. (b) The field distributions for a Gaussian beam incidence deviate from what is expected for homogeneous $\varepsilon = \mu = 0$ medium (Figure 2(a)).

We also remark that linear bands cutting at one point can be found in one-dimensional photonic crystals but it takes a two-dimensional system to define a cone in k-space.

The square lattice has the special property that the group of the M point ($\vec{k}_M = (\pi/a)\hat{x} + (\pi/a)\hat{y}$) is the same as that of Γ point and they both are C_{4v}. Triply degenerate state can again be constructed by arranging for the accidental degeneracy of the two fold degenerate state and one nondegenerate state at the M point. Symmetry analysis shows that we can get a conical dispersion close to the M point, whose dispersion can be written as $\omega(\vec{k}) = \omega_M + v_g|\vec{k} - \vec{k}_M|$ to the first order where ω_M is the frequency of the triply degenerate state, v_g is the group velocity of the linear band. Along with the conical dispersion, an extra band intersects the conical dispersion at ω_M. As we show in Figure 5(a), linear dispersion can indeed be constructed at the M point if there is accidental degeneracy while the dispersion is quadratic if the degeneracy comes from lattice symmetry [71]. To illustrate this point, the dispersion of photonic crystal with an alumina vein structure for the TE polarization is shown in Figure 5(a). As the Dirac-like cone appears at a zone boundary point M, we should not expect effective medium theory to be applicable, and the wave guiding property (Figure 5(b)) is indeed different from what is expect from a homogeneous $\varepsilon = \mu = 0$ medium. In addition, we can also

use vein-like structures to achieve Dirac-like cone dispersion at Γ point, which corresponds to a large square hole drill inside background medium. Again, the low-lying bands of that type of structures cannot be described by monopole and dipole excitations and the system cannot be mapped to a homogeneous $\varepsilon = \mu = 0$ medium even if there is conical dispersion.

The above discussions show that Dirac-like cone dispersion at the Γ point is a necessary condition to obtain $\varepsilon = \mu = 0$ but it is not a sufficient condition. The $\varepsilon_{\text{eff}} = \mu_{\text{eff}} = 0$ property is a special property of some (but not all) photonic crystals with conical dispersion. We note that other intriguing wave transport properties such as pseudo-diffusive transmission [17, 18] and Zitterbewegung [20, 33] are properties of the conical dispersion and can be observed as long as there is a cone, irrespective of whether effective parameters are retrievable or not.

3. The Berry Phase of Dirac-Like Point with Triply Degenerate State

In the above discussion, we considered the relationship between Dirac-like point and zero-index material. The zero-index property is related to a triply degenerate state, with a flat band of a quasi-longitudinal mode crossing the Dirac-like point formed by cones generated by two linear bands. At a first glance, the longitudinal flat band with a zero group velocity in homogeneous material has no role in the Dirac-like point physics and in the literature, there are indeed calculations that ignored the longitudinal mode at all [65]. Even though the longitudinal mode inside the zero-index material cannot be excited by incident plane waves and hence do not participate in the wave transport for some cases, its existence does have some subtle effects. For example, if this longitudinal mode is ignored, the modes near the Dirac-like point can be described by a 2×2 Hamiltonian which can be mapped to the Hamiltonian of a spinor, and such systems can potentially carry a nonzero Berry phase [78, 79]. On the other hand, the triple degenerate state is similar to the spin 1 system [78, 79] and the Berry phase should be zero. Therefore, the existence of the longitudinal state changes the Berry phase of the Dirac-like point which bears implication when we consider effects such as coherent backscattering of light [80] when disordered is introduced. Since our zero-index materials correspond to the accidental degeneracy of the monopole and dipole, it is convenient to use the multiple scattering theory (MST) to calculate the Berry phase, as will be sketched below.

The MST equation can be written as [66]

$$\begin{pmatrix} S_0 - \dfrac{1}{D_{-1}} & -S_1 & S_2 \\ -S_{-1} & S_0 - \dfrac{1}{D_0} & -S_1 \\ S_{-2} & -S_{-1} & S_0 - \dfrac{1}{D_1} \end{pmatrix} \begin{pmatrix} b_{-1} \\ b_0 \\ b_1 \end{pmatrix} = 0, \tag{5}$$

where D_m and b_m are the T-matrix and Mie scattering coefficients of the angular momentum number m, respectively, and S_m denotes the lattice sum in MST. The mathematical details of the MST method can be found in [66]. We can do a small k expansion for the eigenmodes near the Γ point. As $\delta k \to 0$, $S_0 - 1/D_0$, $S_0 - 1/D_{\pm 1}$, S_1 and S_2 can be written as

$$\begin{aligned} S_0 - \frac{1}{D_0} &\approx i(A_0(\omega) + B(\omega)\delta k^2), \\ S_0 - \frac{1}{D_{\pm 1}} &\approx i(A_1(\omega) + B(\omega)\delta k^2), \\ S_1 &\approx C_1(\omega)\delta k e^{i\phi_k}, \\ S_2 &\approx C_2(\omega, \phi_k)\delta k^2, \end{aligned} \tag{6}$$

where $A_0(\omega)$, $A_1(\omega)$, $B(\omega)$, and $C_1(\omega)$ are all real functions of ω only, and $C_2(\omega, \phi_k)$ is a function of ω and $\phi_k \cdot \phi_k$ is the angle of $\delta\vec{k}$ in the polar coordinate. If there is accidental degeneracy, such that $\omega_m = \omega_d = \omega^*$(here ω_m and ω_d are the eigen frequencies of the monopole and dipole excitations, resp.), we can do a small ω expansion near ω^* and obtain $S_0 - 1/D_0 \approx i(A_0'(\omega^*)(\omega - \omega^*) + B(\omega)\delta k^2)$, where $A_0'(\omega) = \partial A_0(\omega)/\partial\omega$, and $S_0 - 1/D_{\pm 1} \approx i(A_1'(\omega^*)(\omega - \omega^*) + B(\omega)\delta k^2)$, where $A_1'(\omega) = \partial A_1(\omega)/\partial\omega$. By substituting them into (5), we can obtain

$$\begin{pmatrix} i(A_1'(\omega - \omega^*) + B\delta k^2) & -C_1\delta k e^{i\phi_k} & C_2\delta k^2 \\ C_1\delta k e^{-i\phi_k} & i(A_0'(\omega - \omega^*) + B\delta k^2) & -C_1\delta k e^{i\phi_k} \\ -C_2^*\delta k^2 & C_1\delta k e^{-i\phi_k} & i(A_1'(\omega - \omega^*) + B\delta k^2) \end{pmatrix} \cdot \begin{pmatrix} b_{-1} \\ b_0 \\ b_1 \end{pmatrix} = 0. \tag{7}$$

The secular equation of (7) is a cubic equation of $\delta\omega$:

$$\begin{aligned} &-(A_1'\delta\omega + B\delta k^2)^2(A_0'\delta\omega + B\delta k^2) \\ &+ 2(A_1'\delta\omega + B\delta k^2){C_1}^2\delta k^2 + (A_0'\delta\omega + B\delta k^2)|C_2|^2\delta k^4 \\ &- 2\,\mathrm{Im}\left(C_2^* e^{2i\phi_k}\right)C_1^2\delta k^4 = 0, \end{aligned} \tag{8}$$

where $\delta\omega = \omega - \omega^*$. By solving this secular equation, we find three solutions: one is $\omega_1 - \omega^* = 0 + O(\delta k^2)$, which corresponds to a band of quadratic dispersion. The other two solutions are $\omega_{2,3} - \omega^* = \pm v_g\delta k + O(\delta k^2)$, where $v_g = \sqrt{2}|C_1|/\sqrt{A_1'A_0'}$, which corresponds to two bands with linear dispersions that generate a Dirac cone.

Neglecting the δk^2 term, and substitute $\delta\omega = (\sqrt{2}|C_1|/\sqrt{A_1'A_0'})\delta k = v_g\delta k$ into (7) for the accidental degenerate monopole and dipoles, (7) can be written as

$$\begin{pmatrix} iA_1'v_g\delta k & -C_1\delta k e^{i\phi_k} & 0 \\ C_1\delta k e^{-i\phi_k} & iA_0'v_g\delta k & -C_1\delta k e^{i\phi_k} \\ 0 & C_1\delta k e^{-i\phi_k} & iA_1'v_g\delta k \end{pmatrix} \begin{pmatrix} b_{-1} \\ b_0 \\ b_1 \end{pmatrix} = 0. \quad (9)$$

Solving (9), we can obtain the relationships between b_{-1}, b_1 with b_0,

$$b_{-1} = -i\frac{C_1 e^{i\phi_k}}{A_1'v_g}b_0, \qquad b_1 = i\frac{C_1 e^{-i\phi_k}}{A_1'v_g}b_0. \quad (10)$$

The eigenvector of (9) is:

$$|\Phi_k\rangle = \begin{pmatrix} -i\dfrac{C_1 e^{i\phi_k}}{A_1'v_g} \\ 1 \\ i\dfrac{C_1 e^{-i\phi_k}}{A_1'v_g} \end{pmatrix}. \quad (11)$$

Therefore, the Berry phase of the eigenstate $|\Phi_k\rangle$ is

$$\begin{aligned} \oint i\left\langle \Phi_k \mid \nabla_{\vec{k}}\Phi_k \right\rangle \cdot d\vec{k} &= \oint i\begin{pmatrix} i\dfrac{C_1 e^{-i\phi_k}}{A_1'v_g} & 1 & -i\dfrac{C_1 e^{i\phi_k}}{A_1'v_g} \end{pmatrix} \nabla_{\vec{k}} \begin{pmatrix} -i\dfrac{C_1 e^{i\phi_k}}{A_1'v_g} \\ 1 \\ i\dfrac{C_1 e^{-i\phi_k}}{A_1'v_g} \end{pmatrix} \cdot d\vec{k} \\ &= \oint i\begin{pmatrix} i\dfrac{C_1 e^{-i\phi_k}}{iA_1'v_g} & 1 & -i\dfrac{C_1 e^{i\phi_k}}{A_1'v_g} \end{pmatrix} \begin{pmatrix} \dfrac{C_1 e^{i\phi_k}}{A_1'v_g} \\ 0 \\ \dfrac{C_1 e^{-i\phi_k}}{A_1'v_g} \end{pmatrix} \nabla_{\vec{k}}\phi_k \cdot d\vec{k} = 0. \end{aligned} \quad (12)$$

From the above analysis, we can see that the Berry phase is equal to zero, which is caused by the existence of the longitudinal flat band. This result is consistent with the discussion shown in [77].

4. Conclusion

In summary, we show that a Dirac-like point formed by a triply degenerate state can exist at the k-points Γ and M in photonic crystals with C_{4v} symmetry. Such triply degenerate states are consequences of accidental degeneracy, which can be achieved by tuning system parameters. Such systems have linear bands crossing the degeneracy point and these linear bands generate Dirac-like cone dispersions. These conical dispersions are generally accompanied by additional parabolic bands that are very flat at the Dirac-like point. For the special case in which the triply degenerate state is derived from monopole and dipole excitations, the system can be mapped to $\varepsilon_{\text{eff}} = \mu_{\text{eff}} = 0$ material through effective medium theory. For other cases in which the bands near the Dirac-like point are not derived from monopole and dipole excitations, effective medium theory does not apply. Using the multiple scattering theory, we calculate the Berry phase of eigenmodes in the Dirac-like cone when there is accidental degeneracy and the phase is found to be zero. Similarly, we can extend Dirac dispersion and effective medium theory to three dimensions [81, 82].

Acknowledgment

This work is supported by Hong Kong RGC GRF Grant 600311.

References

[1] P. A. M. Dirac, "The quantum theory of the electron," *Proceedings of the Royal Society A*, vol. 117, p. 610, 1928.

[2] K. S. Novoselov, A. K. Geim, S. V. Morozov et al., "Electric field in atomically thin carbon films," *Science*, vol. 306, no. 5696, pp. 666–669, 2004.

[3] K. S. Novoselov, A. K. Geim, S. V. Morozov et al., "Two-dimensional gas of massless Dirac fermions in graphene," *Nature*, vol. 438, no. 7065, pp. 197–200, 2005.

[4] Y. Zhang, Y. W. Tan, H. L. Stormer, and P. Kim, "Experimental observation of the quantum Hall effect and Berry's phase in graphene," *Nature*, vol. 438, no. 7065, pp. 201–204, 2005.

[5] V. P. Gusynin and S. G. Sharapov, "Unconventional integer quantum hall effect in graphene," *Physical Review Letters*, vol. 95, no. 14, Article ID 146801, 2005.

[6] K. S. Novoselov, Z. Jiang, Y. Zhang et al., "Room-temperature quantum hall effect in graphene," *Science*, vol. 315, no. 5817, p. 1379, 2007.

[7] M. I. Katsnelsona, "Zitterbewegung, chirality, and minimal conductivity in graphene," *The European Physical Journal B*, vol. 51, no. 2, pp. 157–160, 2006.

[8] J. Cserti and G. David, "Unified description of Zitterbewegung for spintronic, graphene, and superconducting systems," *Physical Review B*, vol. 74, no. 17, Article ID 172305, 2006.

[9] T. M. Rusin and W. Zawadzki, "Transient Zitterbewegung of charge carriers in mono and bilayer graphene, and carbon nanotubes," *Physical Review B*, vol. 76, Article ID 195439, 2007.

[10] G. David and J. Cserti, "General theory of the Zitterbewegung," *Physical Review B*, vol. 81, Article ID 121417, 2010.

[11] A. H. Castro Neto, F. Guinea, N. M. R. Peres, K. S. Novoselov, and A. K. Geim, "The electronic properties of graphene," *Reviews of Modern Physics*, vol. 81, no. 1, pp. 109–162, 2009.

[12] M. I. Katsnelson, K. S. Novoselov, and A. K. Geim, "Chiral tunnelling and the Klein paradox in graphene," *Nature Physics*, vol. 2, no. 9, pp. 620–625, 2006.

[13] S. V. Morozov, K. S. Novoselov, M. I. Katsnelson et al., "Strong suppression of weak localization in graphene," *Physical Review Letters*, vol. 97, no. 1, Article ID 016801, 2006.

[14] A. K. Geim and A. H. MacDonald, "Graphene: exploring carbon flatland," *Physics Today*, vol. 60, no. 8, pp. 35–41, 2007.

[15] A. K. Geim and K. S. Novoselov, "The rise of graphene," *Nature Materials*, vol. 6, no. 3, pp. 183–191, 2007.

[16] M. Plihal and A. A. Maradudin, "Photonic band structure of two-dimensional systems: the triangular lattice," *Physical Review B*, vol. 44, no. 16, pp. 8565–8571, 1991.

[17] R. A. Sepkhanov, Y. B. Bazaliy, and C. W. J. Beenakker, "Extremal transmission at the Dirac point of a photonic band structure," *Physical Review A*, vol. 75, no. 6, Article ID 063813, 2007.

[18] M. Diema, T. Koschny, and C. M. Soukoulis, "Transmission in the vicinity of the Dirac point in hexagonal photonic crystals," *Physica B*, vol. 405, no. 14, pp. 2990–2995, 2010.

[19] R. A. Sepkhanov, J. Nilsson, and C. W. J. Beenakker, "How to detect the pseudospin-1/2 Berry phase in a photonic crystal with a Dirac spectrum," *Physical Review B*, vol. 78, Article ID 045122, 2008.

[20] X. Zhang, "Observing Zitterbewegung for photons near the Dirac point of a two-dimensional photonic crystal," *Physical Review Letters*, vol. 100, no. 11, p. 113903, 2008.

[21] S. Raghu and F. D. M. Haldane, "Analogs of quantum Hall effect edge states in photonic crystals," *Physical Review A*, vol. 78, Article ID 033834, 2008.

[22] F. D. M. Haldane and S. Raghu, "Possible realization of directional optical waveguides in photonic crystals with broken time-reversal symmetry," *Physical Review Letters*, vol. 100, Article ID 013904, 2008.

[23] T. Ochiai and M. Onoda, "Photonic analog of graphene model and its extension: Dirac cone, symmetry, and edge states," *Physical Review B*, vol. 80, no. 15, p. 155103, 2009.

[24] T. Ochiai, "Topological properties of bulk and edge states in honeycomb lattice photonic crystals: the case of TE polarization," *Journal of Physics*, vol. 22, no. 22, p. 225502, 2010.

[25] E. Yablonovitch, "Inhibited spontaneous emission in solid-state physics and electronics," *Physical Review Letters*, vol. 58, no. 20, pp. 2059–2062, 1987.

[26] S. John, "Strong localization of photons in certain disordered dielectric superlattices," *Physical Review Letters*, vol. 58, no. 23, pp. 2486–2489, 1987.

[27] K. M. Ho, C. T. Chan, and C. M. Soukoulis, "Existence of a photonic gap in periodic dielectric structures," *Physical Review Letters*, vol. 65, no. 25, pp. 3152–3155, 1990.

[28] Z. Wang, Y. D. Chong, J. D. Joannopoulos, and M. Soljacic, "Reflection-free one-way edge modes in a gyromagnetic photoniccrystal," *Physical Review Letters*, vol. 100, no. 1, p. 013905, 2008.

[29] Z. Yu, G. s Veronis, Z. Wang, and S. Fan, "One-way electromagnetic waveguide formed at the interface between a plasmonic metal under a static magnetic field and a photonic crystal," *Physical Review Letters*, vol. 100, no. 2, p. 023902, 2008.

[30] Z. Wang, Y. Chong, J. D. Joannopoulos, and M. Soljačić, "Observation of unidirectional backscattering-immune topological electromagnetic states," *Nature*, vol. 461, no. 7265, pp. 772–775, 2009.

[31] X. Ao, Z. Lin, and C. T. Chan, "One-way edge mode in a magneto-optical honeycomb photonic crystal," *Physical Review B*, vol. 80, no. 3, p. 033105, 2009.

[32] Y. Poo, R. X. Wu, Z. Lin, Y. Yang, and C. T. Chan, "Experimental realization of self-guiding unidirectional electromagnetic edge states," *Physical Review Letters*, vol. 106, no. 9, p. 093903, 2011.

[33] X. Zhang and Z. Liu, "Extremal transmission and beating effect of acoustic waves in two-dimensional sonic crystals," *Physical Review Letters*, vol. 101, no. 26, p. 264303, 2008.

[34] V. G. Veselago, "The electrodynamics of substances with simultaneously negative values of ε and μ," *Soviet Physics Uspekhi*, vol. 10, no. 4, p. 509, 1968.

[35] R. A. Shelby, D. R. Smith, and S. Schultz, "Experimental verification of a negative index of refraction," *Science*, vol. 292, no. 5514, pp. 77–79, 2001.

[36] D. R. Smith, W. J. Padilla, D. C. Vier, S. C. Nemat-Nasser, and S. Schultz, "Composite medium with simultaneously negative permeability and permittivity," *Physical Review Letters*, vol. 84, no. 18, pp. 4184–4187, 2000.

[37] S. Zhang, W. Fan, N. C. Panoiu, K. J. Malloy, R. M. Osgood, and S. R. J. Brueck, "Experimental demonstration of near-infrared negative-index metamaterials," *Physical Review Letters*, vol. 95, no. 13, p. 137404, 2005.

[38] V. M. Shalaev, W. Cai, U. K. Chettiar et al., "Negative index of refraction in optical metamaterials," *Optics Letters*, vol. 30, no. 24, pp. 3356–3358, 2005.

[39] G. Dolling, M. Wegener, C. M. Soukoulis, and S. Linden, "Negative-index metamaterial at 780 nm wavelength," *Optics Letters*, vol. 32, no. 1, pp. 53–55, 2007.

[40] J. B. Pendry, "Negative refraction makes a perfect lens," *Physical Review Letters*, vol. 85, no. 18, pp. 3966–3969, 2000.

[41] N. Fang, H. Lee, C. Sun, and X. Zhang, "Sub-diffraction-limited optical imaging with a silver superlens," *Science*, vol. 308, no. 5721, pp. 534–537, 2005.

[42] J. B. Pendry, D. Schurig, and D. R. Smith, "Controlling electromagnetic fields," *Science*, vol. 312, no. 5781, pp. 1780–1782, 2006.

[43] U. Leonhardt, "Optical conformal mapping," *Science*, vol. 312, no. 5781, pp. 1777–1780, 2006.

[44] D. Schurig, J. J. Mock, B. J. Justice et al., "Metamaterial electromagnetic cloak at microwave frequencies," *Science*, vol. 314, no. 5801, pp. 977–980, 2006.

[45] M. Rahm, D. Schurig, D. A. Roberts, S. A. Cummer, D. R. Smith, and J. B. Pendry, "Design of electromagnetic cloaks and concentrators using form-invariant coordinate transformations of Maxwell's equations," *Photonics and Nanostructures*, vol. 6, no. 1, pp. 87–95, 2008.

[46] T. Yang, H. Chen, X. Luo, and H. Ma, "Superscatterer: enhancement of scattering with complementary media," *Optics Express*, vol. 16, no. 22, pp. 18545–18550, 2008.

[47] H. Y. Chen and C. T. Chan, "Transformation media that rotate electromagnetic fields," *Applied Physics Letters*, vol. 90, no. 24, p. 241105, 2007.

[48] Y. Lai, J. Ng, H. Y. Chen et al., "Illusion optics: the optical transformation of an object into another object," *Physical Review Letters*, vol. 102, no. 25, p. 253902, 2009.

[49] M. Silveirinha and N. Engheta, "Tunneling of electromagnetic energy through subwavelength channels and bends using ε-near-zero materials," *Physical Review Letters*, vol. 97, no. 15, p. 157403, 2006.

[50] M. Silveirinha and N. Engheta, "Design of matched zero-index metamaterials using nonmagnetic inclusions in ε-near-zero media," *Physical Review B*, vol. 75, no. 7, p. 075119, 2007.

[51] M. G. Silveirinha and N. Engheta, "Theory of supercoupling, squeezing wave energy, and field confinement in narrow channels and tight bends using ε near-zero metamaterials," *Physical Review B*, vol. 76, no. 24, p. 245109, 2007.

[52] A. Alu and N. Engheta, "Dielectric sensing in ε-near-zero narrow waveguide channels," *Physical Review B*, vol. 78, p. 045102, 2008.

[53] A. Alu, M. G. Silveirinha, and N. Engheta, "Transmission-line analysis of ε-near-zero–filled narrow channels," *Physical Review E*, vol. 78, no. 1, p. 016604, 2008.

[54] B. Edwards, A. Alu, M. G. Silveirinha, and N. Engheta, "Reflectionless sharp bends and corners in waveguides using ε-near-zero effects," *Journal of Applied Physics*, vol. 105, no. 4, p. 044905, 2009.

[55] R. Liu, Q. Cheng, T. Hand et al., "Experimental demonstration of electromagnetic tunneling through an ε-near-zero metamaterial at microwave frequencies," *Physical Review Letters*, vol. 100, no. 2, p. 023903, 2008.

[56] B. Edwards, A. Alu, M. E. Young, M. Silveirinha, and N. Engheta, "Experimental verification of ε-near-zero metamaterial coupling and energy squeezing using a microwave waveguide," *Physical Review Letters*, vol. 100, no. 3, p. 033903, 2008.

[57] K. Halterman and S. Feng, "Resonant transmission of electromagnetic fields through subwavelength zero- ϵ slits," *Physical Review A*, vol. 78, no. 2, p. 021805, 2008.

[58] R. W. Ziolkowski, "Propagation in and scattering from a matched metamaterial having a zero index of refraction," *Physical Review E*, vol. 70, no. 4, p. 046608, 2004.

[59] S. Enoch, G. Tayeb, P. Sabouroux, N. Guerin, and P. Vincent, "A metamaterial for directive emission," *Physical Review Letters*, vol. 89, no. 21, p. 213902, 2002.

[60] A. Alu, M. G. Silveirinha, A. Salandrino, and N. Engheta, "ε-near-zero metamaterials and electromagnetic sources: tailoring the radiation phase pattern," *Physical Review B*, vol. 75, no. 15, p. 155410, 2007.

[61] J. Hao, W. Yan, and M. Qiu, "Super-reflection and cloaking based on zero index metamaterial," *Applied Physics Letters*, vol. 96, no. 10, p. 101109, 2010.

[62] Y. Jin and S. He, "Enhancing and suppressing radiation with some permeability-near-zero structures," *Optics Express*, vol. 18, no. 16, pp. 16587–16593, 2010.

[63] V. C. Nguyen, L. Chen, and K. Halterman, "Total transmission and total reflection by zero index metamaterials with defects," *Physical Review Letters*, vol. 105, no. 23, p. 233908, 2010.

[64] Y. Xu and H. Chen, "Total reflection and transmission by ε-near-zero metamaterials with defects," *Applied Physics Letters*, vol. 98, no. 11, p. 113501, 2011.

[65] L. G. Wang, Z. G. Wang, J. X. Zhang, and S. Y. Zhu, "Realization of Dirac point with double cones in optics," *Optics Letters*, vol. 34, no. 10, p. 1510, 2009.

[66] X. Huang, Y. Lai, Z. H. Hang, H. Zheng, and C. T. Chan, "Dirac cones induced by accidental degeneracy in photonic crystals and zero-refractive-index materials," *Nature Materials*, vol. 10, no. 8, pp. 582–586, 2011.

[67] M. V. Berry, "Quantal phase factors accompanying adiabatic changes," *Proceedings of the Royal Society of London A*, vol. 392, no. 1802, pp. 45–57, 1984.

[68] Y. Wu, J. Li, Z. Q. Zhang, and C. T. Chan, "Effective medium theory for magnetodielectric composites: beyond the long-wavelength limit," *Physical Review B*, vol. 74, no. 8, p. 085111, 2006.

[69] L. H. Gabrielli, J. Cardenas, C. B. Poitras, and M. Lipson, "Silicon nanostructure cloak operating at optical frequencies," *Nature Photonics*, vol. 3, no. 8, pp. 461–463, 2009.

[70] K. Sakoda, *Optical Properties of Photonic Crystals*, Springer-Verlag, Berlin, Germany, 2nd edition, 2004.

[71] Y. D. Chong, X. G. Wen, and M. Soljacic, "Effective theory of quadratic degeneracies," *Physical Review B*, vol. 77, no. 23, p. 235125, 2008.

[72] K. Sakoda and H. Zhou, "Role of structural electromagnetic resonances in a steerable left-handed antenna," *Optics Express*, vol. 18, no. 26, pp. 27371–27386, 2010.

[73] K. Sakoda and H. Zhou, "Analytical study of two-dimensional degenerate metamaterial antennas," *Optics Express*, vol. 19, no. 15, pp. 13899–13921, 2011.

[74] K. Sakoda, "Dirac cone in two- and three-dimensional metamaterials," *Optics Express*, vol. 20, no. 4, pp. 3898–3917, 2012.

[75] K. Sakoda, "Double Dirac cones in triangular-lattice metamaterials," *Optics Express*, vol. 20, no. 9, pp. 9925–9939, 2012.

[76] T. Inui, Y. Tanabe, and Y. Onodera, *Group Theory and Its Applications in Physics*, Springer, Berlin, Germany, 1990.

[77] J. Mei, Y. Wu, C. T. Chan, and Z. Q. Zhang, "Do linear dispersions of classical waves mean Dirac cones?" *Physical Review B*, vol. 86, p. 035141, 2012.

[78] Z. Lan, N. Goldman, A. Bermudez, W. Lu, and P. Ohberg, "Dirac-Weyl fermions with arbitrary spin in two-dimensional optical superlattices," *Physical Review B*, vol. 84, no. 16, p. 165115, 2011.

[79] B. Dora, J. Kailasvuori, and R. Moessner, "Lattice generalization of the Dirac equation to general spin and the role of the flat band," *Physical Review B*, vol. 84, no. 19, p. 195422, 2011.

[80] E. Akkermans, P. E. Wolf, and R. Maynard, "Coherent backscattering of light by disordered media: analysis of the peak line shape," *Physical Review Letters*, vol. 56, no. 14, pp. 1471–1474, 1986.

[81] J. T. Costa and M. G. Silveirinha, "Mimicking the Veselago-Pendry lens with broadband matched double-negative metamaterials," *Physical Review B*, vol. 84, no. 15, p. 155131, 2011.

[82] C. T. Chan, X. Huang, F. Liu, and Z. H. Hang, "Dirac dispersion and zero-index in two dimensional and three dimensional photonic and phononic systems," *Progress In Electromagnetics Research B*, vol. 44, pp. 163–190, 2012.